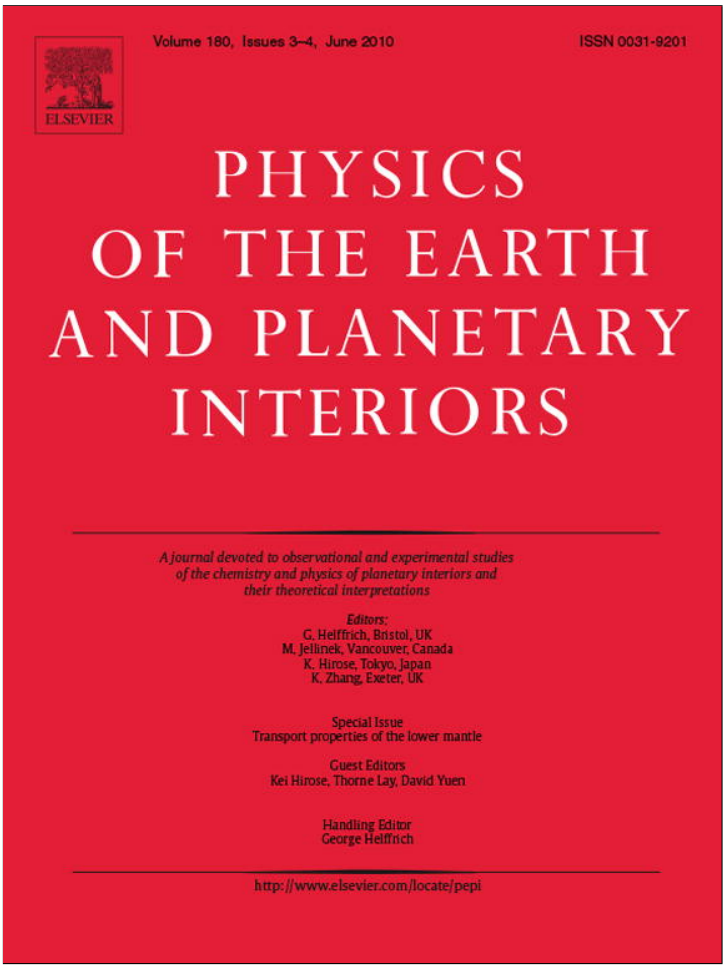

Physics of the Earth and Planetary Interiors 180 (2010) 222–234

Contents lists available at ScienceDirect

Physics of the Earth and Planetary Interiors

journal homepage: www.elsevier.com/locate/pepi

On the interaction of the geotherm with a post-perovskite phase transition in the deep mantle

John W. Hernlund *

Department of Earth and Ocean Sciences, The University of British Columbia, 6339 Stores Road, Vancouver, BC V6T 1Z4, Canada

ARTICLE INFO

Article history:
Received 2 June 2009
Received in revised form 21 January 2010
Accepted 1 February 2010

Guest Editors
Kei Hirose
Thorne Lay
David Yuen

Editor
G. Helffrich

Keywords:
Post-perovskite
Core-mantle heat flow
Mantle convection
Mantle phase transitions
D"

ABSTRACT

The energy balance in the presence of a perovskite (Pv) to post-perovskite (pPv) transition within Earth's D" layer is examined in order to explore the relationship between changes in seismic velocity associated with this phase change, the extent of the two-phase Pv–pPv coexistence region, and the thermal structure of the deep mantle. This is motivated in part by the fact that discontinuities attributed to the Pv–pPv transition are inferred to be seismically sharper than permitted by some recent estimates of the pressure increment across the two-phase co-existence region. Here it is shown that sharp gradients in phase abundance may arise even when the two-phase loop is very broad, and therefore the pressure increment determined from thermodynamic stability alone is a poor proxy for predicting the sharpness of Pv–pPv related seismic discontinuities. The change in pPv fraction over the steepest gradients in phase can also be highly variable, which would lead to potentially complex variations in the total strength of seismic discontinuities. Latent heat plays an important role in the structure of the pPv phase change and its influence upon the geotherm. For the double-crossing scenario – in which a deeper reverse transformation from pPv to Pv occurs in a steep thermal boundary layer – latent heat release from the shallower Pv–pPv transition moderates the effects of latent heat absorption at the deeper reverse transition.

1. Introduction

It is widely recognized that a better determination of the D" layer geotherm would permit an enhanced understanding of the driving forces responsible for convection in the outer core that produces Earth's magnetic field (Braginsky and Roberts, 1995), provide constraints upon lateral temperature variations in the deep mantle that are intimately related to the extent of deep circulation of subducted lithosphere (Schubert et al., 2001), and elicit insights into the nature of any buoyant instabilities in the deep mantle that may give rise to upwelling thermal plumes which rise upward and trace out volcanic hotspot tracks at Earth's surface (Morgan, 1971). Only recently has the discovery of a post-perovskite (pPv) transition in the dominant lower mantle phase $MgSiO_3$ perovskite (Pv) (Murakami et al., 2004; Oganov and Ono, 2004; Tsuchiya et al., 2004a) opened up the possibility of making direct temperature inferences in the D" layer by comparing observations of seismic discontinuities attributed to the Pv–pPv phase change with experimental and ab initio constraints on the position of the phase boundary (Hernlund et al., 2005; Ono and Oganov, 2005; Lay et al., 2006; van der Hilst et al., 2007). These temperature inferences might potentially be used to infer quantities such as CMB heat flux that are central to many of the outstanding questions regarding the evolution of Earth's deep interior (see Lay et al., 2008 for a recent review).

A thermal boundary layer (TBL) exists above the base of Earth's core-mantle boundary (CMB) because conduction down a thermal gradient is the only mechanism capable of accommodating significant radial heat transport out of the surface of the core into the mantle. The surface of the core itself is essentially isothermal, exhibiting lateral temperature variations less than about 10^{-4} K (Braginsky and Roberts, 1995). Variations in temperature and heat flux in the deepest mantle therefore arise exclusively as a consequence of mantle circulation patterns that cool Earth's deep interior, and the core itself plays a strictly passive role by behaving as a sort of heat reservoir with a large thermal inertia. The appearance of pPv-bearing rocks is therefore exclusively controlled by processes operating in the mantle, and its seismic detection and interpretation may lead to important insights into the dynamics of the Earth's deep interior. Additionally, the Pv–pPv phase change has a positive Clapeyron slope, and pPv is stabilized at lower temperatures. Thus pPv-bearing rocks will tend to form in greater abundance within cooler regions of the deep mantle, such as the locations where cool downwellings (e.g., subducted slabs) sink and

* Correspondence address: Department of Earth and Planetary Science, University of California, Berkeley, 307 McCone Hall, Berkeley, CA 94720-4767, USA.
E-mail address: hernlund@gmail.com.

0031-9201/$ – see front matter © 2010 Elsevier B.V. All rights reserved.
doi:10.1016/j.pepi.2010.02.001

pond above the CMB. This makes inferences of temperature using Pv–pPv phase change constraints especially useful because heat transport in the deep mantle is thought to be dominantly controlled by downwellings (e.g., Labrosse, 2002).

Another constraint may be gained from the Pv–pPv phase change because the geotherm may initially pass through the Pv–pPv phase boundary in shallower portions of the D" layer and then revert back to Pv-stability at greater depths inside the TBL if the CMB temperature is greater than the transition temperature at CMB pressure. This has been called the "double-crossing" hypothesis (Hernlund et al., 2005), which offers predictions regarding the seismic velocity structure of the D" layer that can be tested against a variety of seismic data. It was shown more than a decade ago (e.g., Sidorin et al., 1998) that a phase change exhibiting a large Clapeyron slope could best explain the appearance of seismic shear velocity increase discontinuities of up to several percent observed ≈150–300 km above the CMB in some regions (Wysession et al., 1998). If the Pv–pPv phase change (with an estimated Clapeyron slope of order 10 MPa/K) is to account for this velocity increase discontinuity, then a deeper reversion from pPv to Pv will likely be accompanied by a velocity decrease discontinuity (Hernlund et al., 2005). Such a velocity decrease underlying a shallower increase discontinuity has now been reported in numerous studies involving seismic migration beneath Eurasia (Thomas et al., 2004b) and the Cocos-Caribbean region (Thomas et al., 2004a; van der Hilst et al., 2007), waveform modeling beneath the Caribbean (Sun et al., 2006), stacking and inversion of short-period ScS precursors beneath the mid-Pacific (Avants et al., 2006; Lay et al., 2006), and long-period waveform inversion beneath the Cocos-Caribbean region (Kawai et al., 2007a) and Arctic (Kawai et al., 2007b). Furthermore, anti-correlated patterns of P- and S-wave velocity variations that are predicted to occur in pPv elasticity models (e.g., Wookey et al., 2005) have been inferred using seismic data probing D" beneath the Cocos-Caribbean region (Kito et al., 2007; Hutko et al., 2008). Therefore, a variety of seismic techniques thus far support the basic predictions of a Pv–pPv phase change, as well as the occurrence of a double-crossing.

If the Pv–pPv phase change were sensitive to temperature and pressure alone, the double-crossing picture could be expanded to a global scale relatively straightforwardly. For example, because the CMB is isothermal and isobaric, pPv could only occur in lens-like structures above the CMB, and only Pv would be stable at the very base of the mantle (Hernlund et al., 2005). Absence of pPv could then be achieved in some regions as a consequence of a geotherm that is too hot to stabilize pPv. However, large scale variations in bulk composition are almost certainly present in the D" layer, and some of the complex pictures that arise when this is included along with a pPv phase transition have been further explored by Tackley et al. (2007). For example, it has been hypothesized that addition of ferrous iron could have a significant effect, stabilizing pPv inside chemically distinct Fe-rich "piles" that rest at the bottom of the mantle beneath the Pacific and Africa (Lay et al., 2006; Tackley et al., 2007). Spera et al. (2006) studied the form of the pPv double-crossing assuming regular solution in the system $FeSiO_3$–$MgSiO_3$ using early experimental measurements by Mao et al. (2004) and the empirical scaling derived from end-member volume mismatch proposed by Navrotsky (1994). However, the robustness of the pressure standard comparisons of some of these early diamond anvil cell results have since been challenged by Hirose et al. (2006). Indeed, effects involving the system $FeSiO_3$–$MgSiO_3$ that are completely opposite to those reported earlier – with iron destabilizing pPv at lower pressures as opposed to stabilizing it – have since appeared (Tateno et al., 2007). Also, the possibility of a high-spin to low-spin (e.g., Badro et al., 2004) or intermediate-spin (e.g., McCammon et al., 2008) iron transition in perovskite raises further questions about the behavior of Fe at conditions of the deep mantle, and may itself play an unknown but important role in the complex behavior observed in the $FeSiO_3$–$MgSiO_3$ binary system. Additionally, somewhat different perspectives on the partitioning of iron between Pv–pPv and other phases such as ferro-periclase have emerged (e.g., Sinmyo and Ohishi, 2008; Auzende et al., 2008), and this might also have a significant influence on the Pv–pPv phase change. Seismological inferences in support of any of these kinds of scenarios are non-unique, and critically depend upon the mineral physics data and interpretations.

Another emerging issue is that some kinds of compositional effects on the Pv–pPv phase change have been proposed that might substantially broaden the two-phase co-existence region between Pv and pPv, such as the addition of Al_2O_3 (e.g., Akber-Knutston et al., 2005; Catalli et al., 2009). This might complicate the interpretation of discontinuities attributed to the Pv–pPv transition, which exhibit an observed "gradient thickness" of up to around 75 km, corresponding to about 4 GPa in pressure change (e.g., Wysession et al., 1998). The "gradient thickness" is the apparent depth interval over which the majority of the seismic velocity change occurs, and is often assumed to be distributed over the entire two-phase co-existence loop (e.g., Helffrich and Bina, 1994). This viewpoint suggests that any findings of two-phase co-existence with a pressure increment larger than 4 GPa could mean that the Pv–pPv transition cannot not produce discontinuities that are sharp enough to explain the seismic observations. However, the assumption that gradients are always distributed uniformly over the entire two-phase co-existence loop has been shown to be false in the context of shallower mantle phase transitions, because self-consistently calculated phase abundance profiles can be highly non-linear inside the two-phase region, particularly when the two-phase loop is broad (Stixrude, 1997). However, this effect has never been investigated in the context of the Pv–pPv transition, which is significantly different from the shallower phase changes in that it exhibits a relatively large Clapeyron slope, occurs inside a thermal boundary layer, and is potentially influenced by latent heat to a greater extent.

There are also issues related to energy balances for the pPv double-crossing and its implications for heat flux that have not been resolved. One issue is latent heat, which can deflect the geotherm near the phase transition (Verhoogen, 1965). Using a simple heat balance, Buffett (2007) recently showed that latent heat absorption causes a steepening of the geotherm beneath a pPv double-crossing. Essentially, steady production of the higher entropy Pv phase from a lower entropy pPv phase upon downwelling through the lower crossing requires a net input of heat at the phase boundary to balance the absorption of latent heat, which can only be realized by differences in heat conduction (i.e., changes in the thermal gradient) above and below the transition. The implication is a geothermal gradient beneath the pPv lense which is even steeper than that given by a phase boundary gradient lower bound alone. The effect would be enhanced when a two-phase region is present (Buffett, 2007), because the change in conduction needs to additionally balance the difference in advection at the top and bottom owing to the large temperature gradient. This phenomenon possibly provides more leverage on the thermal gradient at the very deepest levels of the mantle, however, it can only be confidently applied if one can rigorously connect kinematic factors such as downwelling velocity with thermodynamic factors such as latent heat and transport properties like thermal conductivity, all of which exhibit a large range of uncertainty.

The relationship between the appearance of pPv-bearing rock and various kinematic or dynamic factors is also an active area of research. Lay et al. (2006) presented simple fits of an error function-like geotherm to observations of discontinuities beneath the central Pacific in an attempt to bracket how uncertainties in the parameters would trade off with the inferred heat flux beneath what was interpreted to be a pPv double-crossing. More ambitious attempts

to relate the deep mantle geotherm to the occurrence of pPv have involved using mantle convection models running under Earth-like parameters along with some approximation of a post-perovskite phase transition (Nakagawa and Tackley, 2004, 2005, 2006; Monnereau and Yuen, 2007; Tackley et al., 2007; Nakagawa and Tackley, 2008). These kinds of studies, performed in both 2D and 3D with domains encompassing the entire mantle, demonstrate that the occurrence of post-perovskite is highly sensitive to parameters governing both the post-perovskite phase boundary as well as those affecting mantle convection. While these kinds of studies ultimately shed light on the connections between the parameters governing the dynamics of mantle convection as well as the appearance and large-scale topology of post-perovskite in relation to convection features, they are necessarily coarsely discretized and cannot shed light on details such as variations in phase abundance inside two-phase regions which are important for interpreting seismological data on a finer scale. The large-scale behavior is, however, important for expansion of temperature and heat flux constraints from the Pv–pPv discontinuity to the entire D" layer. Such efforts also depend upon complementary efforts in seismological mapping of the large-scale occurrence of post-perovskite in the deep mantle, for which some preliminary models and constraints have begun to emerge (e.g., Houser, 2007; Sun and Helmberger, 2008).

The purpose of the present manuscript is to extend earlier work on the Pv–pPv transition to consider the effects of both latent heat evolution and composition variations on the form of the geotherm and the fine-scale distribution of pPv beneath cool downwellings in the deep mantle. Both analytical and numerical techniques are exploited in order to explore the steady-state one-dimensional energy balance and fine structure of the Pv–pPv phase change. The findings are similar to those of Stixrude (1997), and demonstrate that highly non-linear variations in phase may occur when the two-phase loop is broad, and this might help explain why seismically observed gradient thickness of D" discontinuities are smaller than some inferences of the thickness of the two-phase loop. Energy balances across the Pv–pPv transition also demonstrate the importance of latent heat for this phase change, particularly when considered relative to more familiar phase changes at shallower depths in the Earth's mantle.

2. Governing equations

2.1. General form

Conservation of energy can be written as,

$$\frac{\partial(\rho c_p T)}{\partial t} + \vec{\nabla}\cdot\left(\vec{v}\rho c_p T - k\vec{\nabla}T\right) = -T\Delta s\Gamma - \rho g\alpha T v_z + Q + \psi, \qquad (1)$$

where ρ is the density, c_p the specific heat, T the temperature, t the time, $\vec{\nabla}$ the gradient vector, $\vec{v}$ the velocity, k the thermal conductivity, g the acceleration of gravity, α the thermal expansivity, v_z the upward velocity, Δs the entropy change between two phases with Γ measuring the rate of mass conversion from a lower to higher entropy phase per unit volume, Q is the internal heating rate due to radioactive decay, and ψ is the dissipation of energy. Note that in this and the following conventions, Δs is defined so that it is always positive, and the sign of Γ determines whether latent heat is absorbed or released. The pressure P has been assumed to be strictly lithostatic, such that $\vec{\nabla}P = \rho\vec{g}$. The role of internal heating and dissipation on the phase change will not be considered in detail in the present study, and we shall accordingly set $Q = \psi = 0$ in the following developments.

Conservation of mass can be described by,

$$\frac{\partial(\rho_{Pv}\phi)}{\partial t} + \vec{\nabla}\cdot(\vec{v}\rho_{Pv}\phi) = \Gamma, \qquad (2)$$

for the higher entropy Pv phase and,

$$\frac{\partial[\rho_{pPv}(1-\phi)]}{\partial t} + \vec{\nabla}\cdot\left[\vec{v}\rho_{pPv}(1-\phi)\right] = -\Gamma, \qquad (3)$$

for the lower entropy pPv phase, where ϕ is the volume fraction of Pv phase of density ρ_{Pv}, and ρ_{pPv} is the density of the pPv. In this case, pPv is the lower entropy phase and Pv is the higher entropy phase. Note that in taking the volume fraction of pPv phase to be $1-\phi$, the phase change is considered to involve the entire volume of material. This could be compensated for in a partial volume of rock by scaling the entropy change by the appropriate fraction of mantle undergoing the phase change (i.e., $\Delta s \rightarrow f\Delta s$, where f would be the fraction of material undergoing a phase change).

Here I will consider only a binary system in the form of a solid solution that exists in both Pv and pPv. The solute component that is dissolved in solid solution will be denoted by a mole fraction X_{pPv} in pPv and X_{Pv} in Pv. Conservation of solute species leads to the well-known "lever rule," which may be written as:

$$\frac{X - X_{pPv}}{X_{Pv} - X_{pPv}} = \phi\frac{\rho_{Pv}}{\rho}, \qquad (4)$$

where $X = [X_{Pv}\rho_{Pv}\phi + X_{pPv}\rho_{pPv}(1-\phi)]/\rho$ is the composition of the mixture, and $\rho = \rho_{Pv}\phi + \rho_{pPv}(1-\phi)$. The factor ρ_{Pv}/ρ on the right side of Eq. (4) accounts for the small difference between volume and mass fraction, but does not typically differ significantly from unity in the case of Pv and pPv. X is a constant fixed by the chemistry of the rocks, whereas X_{pPv} and X_{Pv} are variable functions of both T and height above the CMB, denoted by the coordinate z.

2.2. Simplifications

The scenario we are interested in here is the case of a pPv lens forming in a downwelling region much wider than it is tall, so that variations in temperature are only significant in the vertical direction z rather than a horizontal direction x. Alternatively, one can assume a vertical axis of symmetry in the middle of a downwelling region, which then reduces to essentially the same mathematical formulation. The basic configuration is illustrated in Fig. 1. For simplicity, we ignore the small contribution of sphericity. In this case

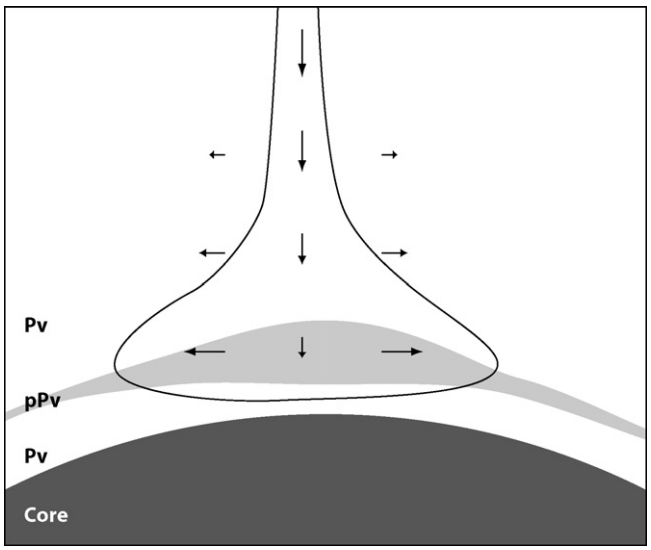

Fig. 1. Schematic illustration of a downwelling flow ponding above the CMB under pure shear deformation giving rise to a region above the CMB where post-perovskite becomes stable owing to a reduced temperature.

the conservation of energy Eq. (1) becomes,

$$\rho c_p \left(\frac{\partial T}{\partial t} + v_z \frac{\partial T}{\partial z} \right) = \frac{\partial}{\partial z} \left(k \frac{\partial T}{\partial z} \right) - T\Delta s\Gamma - \rho g \alpha T v_z, \tag{5}$$

while the conservation of mass Eqs. (2) and (3) become,

$$\rho_{Pv} \left(\frac{\partial \phi}{\partial t} + v_z \frac{\partial \phi}{\partial z} \right) = \Gamma, \tag{6}$$

and,

$$\rho_{pPv} \left[\frac{\partial (1-\phi)}{\partial t} + v_z \frac{\partial (1-\phi)}{\partial z} \right] = -\Gamma. \tag{7}$$

For simplicity, a pure shear style of deformation is adopted, and is described by the velocity field,

$$\vec{v} = v_x \hat{x} + v_z \hat{z} = \dot{\varepsilon}(x\hat{x} - z\hat{z}), \tag{8}$$

where z here is defined as the height above the CMB, $\hat{x}$ and $\hat{z}$ are the unit vectors directed along the coordinates x and z, v_x and v_z are the respective components of velocity, and $\dot{\varepsilon}$ is the strain-rate. Note that the way Eq. (8) is written, $\dot{\varepsilon}$ is positive for downwelling flow. Under this assumed kinematic flow, the 1D conservation of energy Eq. (5) becomes,

$$\rho c_p \left(\frac{\partial T}{\partial t} - \dot{\varepsilon} z \frac{\partial T}{\partial z} \right) = \frac{\partial}{\partial z} \left(k \frac{\partial T}{\partial z} \right) - T\Delta s\Gamma + \rho g \alpha T \dot{\varepsilon} z, \tag{9}$$

while conservation of mass is,

$$\rho_{Pv} \left(\frac{\partial \phi}{\partial t} - \dot{\varepsilon} z \frac{\partial \phi}{\partial z} \right) = \Gamma, \tag{10}$$

and,

$$\rho_{pPv} \left[\frac{\partial (1-\phi)}{\partial t} - \dot{\varepsilon} z \frac{\partial (1-\phi)}{\partial z} \right] = -\Gamma. \tag{11}$$

While this form for the downwelling flow is admittedly simple in form, and a large variety of other circumstances might apply to a pPv lens (e.g., that arising from variable viscosity due to both phase and temperature variations), this formulation allows us to study the most basic behavior of the system while utilizing the fewest parameters.

3. Time dependence and steady state

In most of the models described in this manuscript, a steady-state assumption is adopted in order to simplify the analysis. However, mantle convection is time-dependent, and some consideration of this time-dependence as it applies to the boundary layer is useful in order to assess the magnitude of any error arising from a steady-state assumption. It is useful to begin by finding particular one-dimensional half-space solutions for temperature in the absence of phase changes and adiabatic heating by setting $\Gamma = \alpha = 0$. Here I also take k to be constant. The governing equation for temperature is then,

$$\frac{\partial T}{\partial t} - \dot{\varepsilon} z \frac{\partial T}{\partial z} = \kappa \frac{\partial^2 T}{\partial z^2}, \tag{12}$$

where $\kappa = k/\rho c_p$ is the thermal diffusivity. Most simple descriptions of the thermal boundary layer invoke an error function-like form for the geotherm. This is convenient for a basic analysis of the time dependence of the boundary layer, because a temperature profile assuming the form of an error function is in fact a solution to Eq. (12). With this motivation, it is useful to seek time-dependent solutions to Eq. (12) of the form,

$$\frac{T_{cmb} - T}{T_{cmb} - T_\infty} = erf\left(\frac{z}{z_0} \right), \tag{13}$$

where T_{cmb} is the CMB T, T_∞ is the limiting (potential) temperature far above the CMB, and z_0 is a characteristic length scale of the thermal boundary layer and is itself a function of t (i.e., $z_0 = z_0(t)$). Notice that the temperature drop across the boundary layer, $T_{cmb} - T_\infty$, is constant in this example, so that this kind of functional form only captures variations in the thickness of the boundary layer as it responds to changes in strain-rate. Perturbations in temperature will be considered next. Substituting Eq. (13) into Eq. (12) yields an ordinary differential equation in time for z_0^2,

$$\frac{dz_0^2}{dt} + 2\dot{\varepsilon} z_0^2 = 4\kappa, \tag{14}$$

with the solution,

$$z_0^2 = \frac{z_0^2(t_0) + 4\kappa \int_{t_o}^{t} u(t')dt'}{u(t)}, \tag{15}$$

where,

$$u(t) = \exp\left(2 \int_{t_o}^{t} \dot{\varepsilon}(t')dt' \right), \tag{16}$$

and t_0 is an initial time.

Several interesting features arise from this simple solution for the time dependence of the boundary layer thickness. First, according to Eq. (15), given a constant value of $\dot{\varepsilon}$ the boundary layer thickness z_0 approaches the steady-state value,

$$z_0(t \to \infty) = \sqrt{\frac{2\kappa}{\dot{\varepsilon}}}. \tag{17}$$

The length scale $z_0(t \to \infty)$ is of fundamental importance in the present problem. The physical interpretation of $z_0(t \to \infty)$ is the length scale over which a balance between advection of cool material downward from above and conduction of heat upward from below is maintained. This also gives the appropriate value for the boundary layer thickness whenever a steady-state assumption is adopted. One could also write the above relationship (recalling $|v_z| = z\dot{\varepsilon}$) as,

$$Pe_{z_0} = \frac{|v_z| z_0(t \to \infty)}{\kappa} = 2, \tag{18}$$

where Pe_{z_0} is the Peclet number with the steady-state value of z_0 chosen as the dimensional length scale. This demonstrates the fact that a TBL subject to downwelling from above will strive to achieve an equilibrium thickness z_0 such that the Peclet number is exactly 2. Notice that this offers a constraint on the values that may be assumed by v_z, $z_0(t \to \infty)$, and κ at steady-state, such that choosing any two values determines the magnitude of the other. This is a reduction of the degrees of freedom for the boundary layer problem that is strictly valid only when a steady-state exists.

The foregoing analysis may also be extended to the time-dependence of the geotherm and its relation to the steady state. Consider the case where the temperature is initially that of an error function profile characterized by $z_0(t_i) \neq z_0(t \to \infty)$ at some initial time t_i. From the solution (15) the boundary layer thickness approaches the steady value $z_0(t \to \infty)$ according to,

$$z_0^2(t) = z_0^2(t_i) \exp\left[-2\dot{\varepsilon}(t - t_i) \right] + z_0^2(t \to \infty). \tag{19}$$

This result shows that z_0^2 decays to its steady value $z_0^2(t \to \infty)$ over an e-fold time scale of $1/2\dot{\varepsilon}$. The remarkable feature of this time scale is that it depends in no way on the thermal diffusivity. In cases that do not involve any kind of strain, characteristic time scales of order D^2/κ are more applicable (where D is the relevant length scale). For comparison, a strain-rate of $\dot{\varepsilon}$=10^{-15} s^{-1} typical of mantle deformation yields an equilibration time scale of order tens of millions of years. On the other hand, for this kind of boundary layer process operating over a typical boundary layer length scale of

100 km the thermal diffusion time scale would be of order several hundred million years, i.e., an order of magnitude longer than the strain-rate controlled time scale. The time scale $1/2\dot{\varepsilon}$ determined in this special case is solely representative of the time it takes for a temperature field already in a self-similar error function form to be transformed into another error function form that balances advection and diffusion.

The time scale for the decay of more general kinds of temperature fluctuations of length scale λ can also be evaluated by adding an oscillatory perturbation to temperature of the form $\Theta(t)\sin[2\pi z/\lambda(t)]$, where the amplitude $\Theta(t)$ and wavelength $\lambda(t)$ of the perturbation are both functions of time, and the perturbation is expected to eventually disappear under the action of diffusion. Substituting this into the governing Eq. (12) gives,

$$\left(\frac{4\pi^2\kappa\Theta}{\lambda^2}+\Theta'\right)\sin\left(\frac{2\pi z}{\lambda}\right)-\left(\frac{2\pi\dot{\varepsilon}z\Theta}{\lambda}+\frac{2\pi z\Theta\lambda'}{\lambda^2}\right)\cos\left(\frac{2\pi z}{\lambda}\right)=0, \tag{20}$$

where a prime is used here to denote the time derivative. Requiring the terms proportional to the sine and cosine to vanish independently yields two coupled equations,

$$\Theta'+\frac{4\pi^2}{\lambda^2}\kappa\Theta=0, \tag{21}$$

$$\lambda'+\dot{\varepsilon}\lambda=0. \tag{22}$$

Eq. (22) may be solved to give,

$$\lambda=\lambda_0\exp[-\dot{\varepsilon}(t-t_0)], \tag{23}$$

where λ_0 is the wavelength at an initial time t_0. Θ can then be obtained using Eq. (21),

$$\Theta=\Theta_0\exp\left(-\frac{4\pi^2\kappa[\exp(2\dot{\varepsilon}t)-\exp(2\dot{\varepsilon}t_0)]}{\dot{\varepsilon}\lambda_0^2}\right), \tag{24}$$

where Θ_0 is the initial amplitude of the temperature perturbation. The time scale required to reduce the amplitude of the perturbation by a factor 1/e is given by,

$$\tau=\frac{1}{2\dot{\varepsilon}}\log\left[1+\frac{\dot{\varepsilon}}{\kappa}\left(\frac{\lambda_0}{2\pi}\right)^2\right], \tag{25}$$

which is, once again, of leading order $1/2\dot{\varepsilon}$ because $(\dot{\varepsilon}/\kappa)(\lambda_0/2\pi)^2$ is of order unity for typical parameters and therefore does not substantially affect the logarithmic term (this is true even for large variations of these parameters around typical values). The reason for the dominance of shear on time scales in the present scenario is that in a pure shear-style shortening the wavelength of a temperature variation decreases exponentially in time according to Eq. (23), and while the amplitude decays slowly when the wavelength is large, it begins to decay very rapidly once λ has decreased sufficiently enough to make diffusion highly efficient. Therefore it is reasonable to suggest that in all cases for the present problem the relevant time scale for the geotherm to reach a steady-state is always $1/2\dot{\varepsilon}$. This time scale is the same as the time required for downwelling material to transit the boundary layer and become incorporated into the very bottom of the mantle, such that soon after a slab arrives and ponds above the CMB nearly steady-state geothermal conditions will be realized.

4. Steady energy balance for the post-perovskite double-crossing

Here we turn to the influence of latent heat across both a Pv→ pPv phase change as well as the pPv→ Pv transition that occurs at greater depths in the thermal boundary layer in the double-crossing scenario. This problem is similar to the one addressed by Buffett (2007) for the lower crossing, but is arrived at in a slightly different manner and here we will include a finite transition width in the analysis. For simplicity, in this section I assume that the contribution of adiabatic heating inside the two-phase region is negligible in comparison to latent heat (i.e., $\alpha=0$). At steady-state conditions Eqs. (1)–(3) give,

$$\frac{\partial}{\partial z}\left(\rho v_z c_p T-k\frac{\partial T}{\partial z}\right)=-T(\Delta s\Gamma), \tag{26}$$

$$\frac{\partial}{\partial z}(\rho v_z\phi)=\Gamma, \tag{27}$$

$$\frac{\partial}{\partial z}[\rho v_z(1-\phi)]=-\Gamma. \tag{28}$$

There exist two cases for the double-crossing: one in which the higher entropy Pv phase appears above the region hosting the lower entropy pPv phase (upper crossing) and one in which the higher entropy Pv phase appears below the region hosting the lower entropy pPv phase (lower crossing). Apart from differences in the magnitude of the Clapeyron slope, the upper crossing is similar to other well-studied exothermic phase changes, such as olivine→ β-spinel (e.g., Schubert et al., 2001). On the other hand, the lower crossing case does not have simple analogies in other settings and therefore has not been studied in detail, with the exception of the study of Buffett (2007).

Let the two-phase region (for either the upper or the lower crossing) be confined to some coordinate range $z^-\le z\le z^+$, and for convenience of notation let a super-script "−" or "+" raised over a variable denote the value of that variable at $z=z^-$ or $z=z^+$, respectively. For example, $\phi(z=z^-)=\phi^-$ and $\phi(z=z^+)=\phi^+$ are the values of ϕ (the fraction of Pv phase) at the bottom and top of the two-phase region, respectively. For the upper crossing, notice that $\phi^-=0$ and $\phi^+=1$ (i.e., Pv is absent at the bottom of the two-phase region). On the other hand, for the lower crossing, $\phi^-=1$ and $\phi^+=0$ (i.e., Pv is absent at the top of the two-phase region). Using this shorthand notation, integrating Eqs. (26) and (27) from z^- to z^+ gives,

$$\left(\rho^+v_z^+c_p^+T^+-k^+\left[\frac{\partial T}{\partial z}\right]^+\right)-\left(\rho^-v_z^-c_p^-T^--k^-\left[\frac{\partial T}{\partial z}\right]^-\right)=-\int_{z^-}^{z^+}T\Delta s\Gamma dz, \tag{29}$$

and,

$$\rho^+v_z^+\phi^+-\rho^-v_z^-\phi^-=\int_{z^-}^{z^+}\Gamma dz. \tag{30}$$

From integration by parts,

$$\int_{z^-}^{z^+}T\Delta s\Gamma dz=\int_{z^-}^{z^+}T\Delta s\frac{\partial}{\partial z}(\rho v_z\phi)dz=[T\Delta s\rho v_z\phi]_{z^-}^{z^+}-\int_{z^-}^{z^+}\frac{\partial(T\Delta s)}{\partial z}\rho v_z\phi dz. \tag{31}$$

If changes in ρv_z across the two-phase region are negligibly small, then we can write,

$$\int_{z^-}^{z^+}T\Delta s\Gamma dz=\mp\overline{T\Delta s}\rho|v_z|, \tag{32}$$

where $v_z < 0$ is assumed and,

$$\pm\overline{T\Delta s} = [T\Delta s\phi]_{z^-}^{z^+} - \int_{z^-}^{z^+} \frac{\partial(T\Delta s)}{\partial z}\phi dz, \tag{33}$$

is the effective latent heat of the transition. The $\mp$ and $\pm$ signs appearing in these expressions are applied as follows: the upper sign is for the upper crossing case and the lower sign is for the lower crossing case (this sign convention will continue to be used below). Note that the integral term in Eq. (33) is usually neglected in most analyses because its relative importance is of order $(T^+ - T^-)/T$. The energy balance obtained by integrating over the two-phase region may then be written as,

$$-\rho|v_z|\left(c_p^+T^+ - c_p^-T^-\right) - k^+\left[\frac{\partial T}{\partial z}\right]^+ + k^-\left[\frac{\partial T}{\partial z}\right]^- = \pm\overline{T\Delta s}\rho|v_z|. \tag{34}$$

The assumptions leading to Eq. (34) should be re-iterated: adiabatic heating and internal heating, as well as variations in ρv_z have all been neglected over the depth range encompassing the two-phase region, and the velocity is assumed to be in the downward direction.

When all phases are well above their Debye temperatures and non-linear mode coupling due to anharmonicity is negligible, we can take $c_p^+ = c_p^- = c_p$. If we also assume that the thermal conductivity does not differ significantly between the two-phases (i.e., $k^+ = k^- = k$), then the difference in temperature gradients above and below the two-phase region can be written:

$$\left[\frac{\partial T}{\partial z}\right]^+ - \left[\frac{\partial T}{\partial z}\right]^- = \frac{|v_z|}{\kappa}\left(\mp\frac{\overline{T\Delta s}}{c_p} \mp \Delta T_{inc} + \frac{\rho g}{\gamma}\delta\right). \tag{35}$$

where κ is the thermal diffusivity, ΔT_{inc} is the positive temperature increment across the two-phase loop at constant pressure for a given bulk composition, g is the gravitational acceleration, γ is the Clapeyron slope, and $\delta = z^+ - z^-$ is the depth interval of the two-phase region. In writing Eq. (35) I used the relation between the total temperature change across the two-phase region, $T^- - T^+$, and the pressure dependence of the phase diagram given by the Clapeyron relation, to find,

$$T^- - T^+ = \pm\Delta T_{inc} + \frac{\rho g\delta}{\gamma}. \tag{36}$$

This relation is illustrated in Fig. 2, which shows how the phase diagram is shifted down or up in temperature at the upper and lower extents of the two-phase regions, respectively, for both the upper and lower crossing scenarios and a given bulk composition. In writing Eq. (36) I have assumed that the change in pressure across the two phase region does not significantly change the form of the phase diagram in temperature-composition space. In other words, the assumption is that only effect of pressure change across the two-phase region is to shift the phase diagram up or down in temperature by a magnitude given solely by the Clapeyron relation.

Some insights may be obtained for the Pv→ pPv transition by exploiting limiting circumstances in order to simplify the above relations. When advection is more important than diffusion (i.e., in the limit $|v_z|/\kappa \to \infty$), the left side of Eq. (36) vanishes and it is straightforward to solve for the two-phase region thickness,

$$\delta = \delta_{lat} + \delta_{comp} = \left(\frac{T}{gc_p}\right)\left(\frac{\Delta\rho}{\rho}\right)\left(\frac{\gamma}{\rho}\right)^2 + \left(\frac{\Delta T_{inc}}{g}\right)\left(\frac{\gamma}{\rho}\right), \tag{37}$$

where $(\Delta\rho/\rho)\gamma/\rho$ has been substituted for Δs by means of the Clapeyron relation. The first term, δ_{lat}, is the contribution to the transition depth interval due only to deflection of the geotherm along the phase boundary by latent heat release. Note that this baseline depth interval over the two-phase region applies even in the case of a univariant transition. The second term, δ_{comp}, is the contribution to the phase transition depth increment owing to composition influences upon the phase equilibrium, and accordingly scales with the temperature increment across the two-phase region, ΔT_{inc} (notice that $\Delta T_{inc}\gamma = \Delta P_{inc}$, the corresponding pressure increment across the two-phase loop). The δ_{lat} obtained here by assuming $|v_z|/\kappa \to \infty$ is an upper bound, and this value can be much smaller when thermal diffusion is important (e.g., Schubert et al., 2001).

It is interesting to compare how δ_{lat} and δ_{comp} differ for the case of the Pv–pPv transition relative to more familiar transition zone phase changes. For a transition zone phase change exhibiting γ of order 1 MPa/K, $\rho = 3300\,\mathrm{kg/m^3}$, $\Delta\rho/\rho$=1%, $g = 10\,\mathrm{m/s^2}$, and $c_p = 1000\,\mathrm{J/kg/K}$, this calculation gives δ_{lat} of order 1 km. For the same kind of phase transition including a variance in composition and using a temperature increment across the two-phase loop of $\Delta T_{inc} = 100$ K yields δ_{comp} of about 3 km. Thus the transition width is increased by a factor of 4 in this case when ΔT_{inc} is increased from 0 to 100 K. On the other hand, in a Pv→ pPv phase change with T =2000 K, $\rho = 5000\,\mathrm{kg/m^3}$ and γ of order 10 MPa/K (keeping other parameters the same as above), we find that δ_{lat} is around 100 km. This is much larger than the transition zone value of δ_{comp}, owing mostly to the quadratic dependence upon γ. Adding a ΔT_{inc} of 100 K in the Pv→ pPv case gives δ_{comp} of around 40 km. Notice that $\delta_{comp}/\delta_{lat}$ is about one order

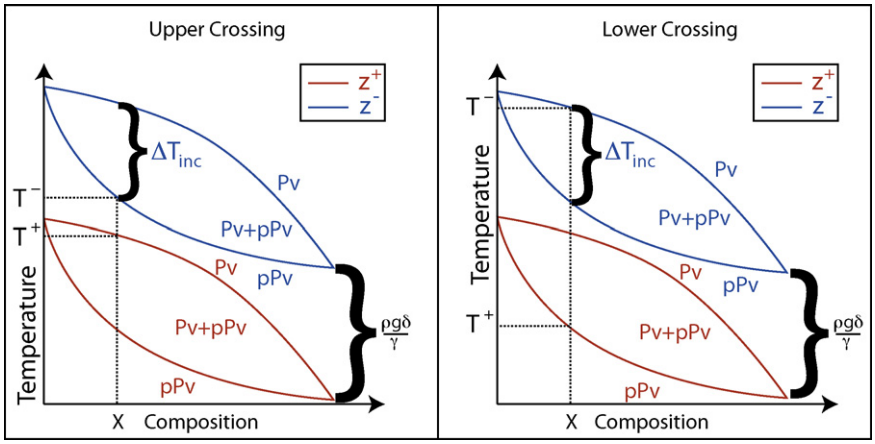

Fig. 2. Illustration of the relationship between T^+, T^-, ΔT_{inc} and $\rho g\delta/\gamma$. The temperature of the binary loop is higher for the height z^- at the base of the two-phase region relative to the height z^+ at the top of the two-phase region.

of magnitude smaller for the Pv→ pPv case relative to the "typical" transition zone phase change considered above. While one shouldn't expect the limit $|v_z|/\kappa \to \infty$ to apply exactly in the upper crossing scenario, in particular due to its proximity to the TBL and corresponding influence of at least some changes in thermal gradient, these numbers are still useful as a guide for relative variations in the nominal widths of the phase transition. In particular, these numbers demonstrate that latent heat plays a relatively more important role in the Pv→ pPv phase change than it does in more familiar transition zone phase changes, and care should be taken in applying approximations that may be valid for the latter cases but not in the former case. Additionally, the depth increment expected across the Pv→ pPv phase change is intrinsically much larger than shallower phase changes with smaller Clapeyron slopes.

For the lower crossing scenario, if $\Delta T_{inc} = \delta = 0$ (as in the case of an infinitesimally thin, univariant transition), then Eq. (35) reduces to exactly the same expression obtained previously by Buffett (2007). It appears that, for a univariant phase change, the contribution of latent heat to the transition width, δ_{lat}, can indeed be nil. Also, in the lower-crossing case the terms proportional to $|v_z|/\kappa$ are all positive, and a change in thermal gradient across the transition is inevitable according to Eq. (35). The physical significance of this expression for the lower crossing is that the absorption of latent heat in converting the lower entropy pPv phase to the higher entropy Pv phase is balanced by differences in heat conduction into the two phase region on either side of the phase boundary. For the lower crossing, the magnitude of the thermal gradient is greater below the transition than above the transition. Note, however, that the difference in temperature gradients is larger for the lower crossing when a two-phase region is present and $\Delta T_{inc} \neq 0$ (Buffett, 2007). In this case, the increased net conduction of heat into the two-phase region must also accomodate the fact that material leaving the region is hotter than when it entered by an amount $T^- - T^+$, which yields a net divergence in advected heat flux that must also be balanced by an even larger change in thermal gradients above and below the two-phase region. Eq. (35) may be used to estimate the relative importance of these effects. We will return to this subject in the next section, where inclusion of both the upper and lower crossings is found to moderate the overall influence of this geothermal steepening effect. However, this kind of steepening will still imply a lower bound for the geothermal gradient beneath a pPv double-crossing that is larger than the gradient of the phase boundary by an amount equal to the right-side of Eq. (35). If the thermal conductivity is known, then this can provide potentially very useful constraints upon the CMB heat flux where ever a pPv double-crossing occurs in the deep mantle.

5. Numerical solutions

Next we turn to steady-state numerical solutions of Eq. (9). As with all previous sections internal heating is neglected, however, in the present solutions adiabatic heating is included for purposes of illustration. It will be seen that the effect of adiabatic heating is to introduce a gradual gradient in temperature that is only significant over many hundreds of km, and it does not affect the structure of the phase change itself. Numerical solutions are obtained with relative ease using the finite-difference method, which for a standard second-order discretization produces a tri-diagonal system of equations that is solved with negligible computational expense. This numerical method is useful for exploring the complexities of both the temperature and pPv abundance inside the boundary layer under various conditions, where many of the kinds of assumptions that allow for straightforward analytical solutions do not always yield sufficiently accurate results.

5.1. Model definitions and parameters

It is important to recognize that the problem of solving for phase abundance and/or temperature is inherently non-linear due to the coupling between phase production, the phase diagram, and latent heat. If phase production is changed, it will cause a deflection in the geotherm owing to the corresponding change in latent heat production. Yet the deflection in the geotherm itself will cause a shift in the equilibrium which, in turn, affects the abundance of phases. In the present nomenclature, Γ may be obtained directly using the mass conservation Eq. (2) if variations in ϕ are known. However, ϕ itself depends on the phase diagram and the temperature. The approach I use here is to begin by first assuming $\Gamma = 0$, obtain a solution for T given all the other parameters, and then use this T to calculate ϕ using the imposed phase diagram and lever rule Eq. (4). Then Γ is obtained using Eq. (2) and the initial solution for ϕ, and is subsequently used to update the solution for T via another solution of the energy equation using the first estimate of Γ. This procedure is continued recursively until convergence to the full non-linear solution.

For the phase diagram I adopt a simplified binary phase loop for practical purposes. In particular, the lower and upper temperature limits of the binary phase loop in the models vary according to,

$$T = \frac{\Delta T_{inc}}{2}\frac{X_{pPv}(1-X_{pPv})}{X_0(1-X_0)} + T_0 - X_{pPv}(T_0 - T_1) \tag{38}$$

and,

$$T = -\frac{\Delta T_{inc}}{2}\frac{X_{Pv}(1-X_{Pv})}{X_0(1-X_0)} + T_0 - X_{Pv}(T_0 - T_1)\,. \tag{39}$$

Here, ΔT_{inc} is (as in previous sections) defined as the temperature increment across the two-phase loop at a fixed reference bulk composition X_0. T_0 and T_1 are the temperatures of the univariant transitions at the end member compositions $X = 0$ and $X = 1$, respectively. T_0 and T_1 are both a function of pressure, and vary according to,

$$T_0 = T_{0,cmb} + (P - P_{cmb})\gamma, \tag{40}$$

and,

$$T_1 = T_{1,cmb} + (P - P_{cmb})\gamma, \tag{41}$$

where P is the pressure and P_{cmb} is the CMB pressure. This formulation yields a simplified binary phase loop of the kind that would arise when there is continuous solid solution of a pair of components in both phases, and its analytical simplicity is convenient for use in the computations carried out here. While more realistic thermodynamical models are desirable, these introduce more parameters and at present there are too few constraints to make them more useful than a generic description. Indeed, it is not even certain whether there exists a continuous two-phase binary solid solution loop for various components that are relevant to a Pv–pPv equilibrium. Thus in the context of the present study, exploring model space in terms of any particular thermodynamic model is premature. The simplified phase diagram adopted here is illustrated in Fig. 3. Since P and P_{cmb} are known, the basic form of the phase diagram in this case depends only on the parameters γ, ΔT_{inc}, X_0, $T_{0,cmb}$ and $T_{1,cmb}$. Note that the pressure increment of the two-phase loop ΔP_{inc} can be obtained using $\Delta P_{inc} = \Delta T_{inc}\gamma$, while the depth increment at constant temperature Δz_{inc} is given by $\Delta z_{inc} = \Delta T_{inc}\gamma/\rho g$.

There exist many potential candidates for the range of composition variations in both Pv and pPv. Important solid solution series might include the $FeSiO_3$–$MgSiO_3$ binary, and/or systems involving various kinds of substitutions of Al_2O_3 (which may or may not involve changes in Fe oxidation state). In the present models, the

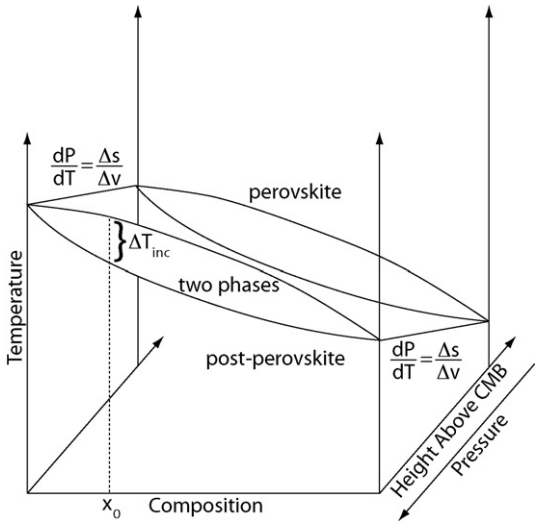

Fig. 3. Perspective sketch of the kind of phase diagram considered in this study. The form of the phase diagram in the T–X plane does not vary with pressure apart from an upward or downward shift that follows the Clapeyron relation.

generic fraction X is taken to be the solute representative of the non-$MgSiO_3$ component in a given solution series, such as the fraction of $FeSiO_3$ in either Pv or pPv. Thus X is of order 10%, representative of abundances of these oxides in the mantle. This means that the composition in either phase will always be near the $MgSiO_3$ end-member. Because the boundaries of the two-phase loop converge at the end-member, and diverge in the direction of increasing X, there is a basic form imposed upon the relevant portion of the phase diagram. Thus a smaller value of X may be compensated by an increase in ΔT_{inc}, and similar behavior would be obtained because the compositions still remain close the the edge of the binary phase loop.

Note that in this model the addition of solute X may either stabilize pPv or Pv, depending on the relative values of $T_{0,cmb}$ and $T_{1,cmb}$. If addition of X favors formation of pPv at constant temperature ($T_{0,cmb} < T_{1,cmb}$), then component X may be said to stabilize pPv at lower pressures relative to the $MgSiO_3$ end-member. If, on the other hand, addition of X favors formation of Pv at constant temperature ($T_{0,cmb} > T_{1,cmb}$), then component X may be said to shift the phase change to higher pressures. Either behavior is possible for the Pv–pPv phase change.

For the thermal conductivity a typical phonon-dominated model is employed, and varies like $k = k_{cmb}(T_{cmb}/T)$, where k_{cmb} is the thermal conductivity of rock at the CMB temperature T_{cmb}. A relatively low value of $k_{cmb} = 5$ W/m/K is adopted, consistent with the phonon contribution to k that motivates the form of the function $k(T)$. Radiative contributions to thermal conductivity are very poorly constrained in the deep mantle, and are ignored in the present models. The density and gravity are taken directly from the PREM model (Dziewonski and Anderson, 1981). The specific heat is assumed to be constant at a value of 1200 J/K/kg. The reference value for the Clapeyron slope is taken to be $\gamma = 13$ MPa/K, a value now favored by a reconciliation of numerous laser-heated diamond anvil cell (LHDAC) experiments to a common MgO pressure standard (Hirose et al., 2006; Hirose, 2006; Tateno et al., 2009), and which is consistent with plausible temperatures implied in the core for a pPv double-crossing (Hernlund and Labrosse, 2007). The nominal value of the volume change Δv is taken to be independent of composition and is usually set at 1%, although we explore other values below. Δs is computed by using the Clapeyron relation $\Delta s = \Delta v \gamma$, thus varying Δv leads to a proportional variation in Δs. Thermal expansivity, which affects only the adiabatic gradient, is set to a constant value of 5×10^{-6} K^{-1}. Although the adiabatic gradient is not found to be important, it is included here for illustrative purposes. The CMB temperature is taken to be $T_{cmb} = 4000$ K, and the temperature 1000 km above the CMB is set to 2500 K. The nominal value of the strain-rate is taken to be $\dot{\varepsilon} = 2 \times 10^{-16}$ s^{-1}, but this is also varied. For ΔT_{inc}, X_0, $T_{0,cmb}$ and $T_{1,cmb}$ governing the basic form and position of the phase diagram, we take as our nominal values $\Delta T_{inc} = 300$ K, X_0=0.15, $T_{0,cmb} = 2600$ K and $T_{1,cmb} = 3600$ K. These parameters correspond to a pressure increment $\Delta P_{inc} = 3.9$ GPa (depth increment $\Delta z_{inc} = 69$ km) at constant temperature. For these relative values of $T_{0,cmb}$ and $T_{1,cmb}$, the addition of the solute represented by the fraction X shifts the equilibrium in the direction of Pv when pressure and temperature are held constant. Cases are also performed with the relative variation reversed, so that addition of solute X stabilizes pPv. The above parameter values are summarized in Table 1.

Table 1
Parameter values considered in this study.

Quantity	Value (range, if applicable)
ρ_{Pv}	5500 kg/m^3
g	10.3 m/s^2
γ	13 MPa/K
ΔV	1 (1–4)%
ΔT_{inc}	300 (200–500) K
$\dot{\varepsilon}$	2×10^{-16} ($10^{-16.5}$–10^{-15}) sec^{-1}
T_{cmb}	4000 K
T_∞	2500 K
k_{cmb}	5 W/m/K
c_p	1200 J/K/kg
X_0	0.15
$T_{0,cmb}$	3600,3600 K
$T_{1,cmb}$	2600,4600 K

Values of parameters, and their ranges (if applicable), used in the numerical solutions presented in Figs. 4–7.

5.2. Model results

Fig. 4 shows the effect of strain-rate variations on the form of the solution obtained for the geotherm and fraction of pPv. These are cases where $T_{0,cmb} = 3600$ K and $T_{1,cmb} = 2600$ K, such that addition of X stabilizes Pv. As predicted earlier in Eq. (17), the length scale, or thickness, of the boundary layer at steady conditions varies inversely to $\sqrt{\dot{\varepsilon}}$, such that the boundary layer is compressed for higher values of $\dot{\varepsilon}$. This behavior is straightforward, and varies little from what we already obtained using analytical solutions. This example shows that pPv can be completely absent if the downwelling flow is weak and the thermal boundary layer is thick, even though the temperatures high above the TBL are equal in all cases. As the boundary layer thins with higher strain-rate, the geotherm dips into the two-phase region and pPv is formed. However, for a geotherm that enters only the two-phase region, but does not pass into the Pv-free region to produce a Pv-free "core," there is a smooth variation in pPv fraction and there is no clear distinction between an upper and lower crossing. Still, the pPv abundance profile is nonlinear, and large gradients in phase exist at the top and bottom of the pPv-bearing region, such that a positive and negative discontinuity could still be produced at the top and bottom of the pPv-bearing region. Using seismology alone, it might be difficult to distinguish this case from those where a Pv-free core forms between the upper and lower crossing, because both produce positive and negative discontinuities. However, the total change in phase abundance accross the steepest gradient could be smaller if the geotherm barely enters the Pv–pPv co-existence region, which would lead to a weaker apparent discontinuity in seismic velocity. Latent heat deflection is the only effect that causes the geotherm to differ substantially in appearance from a simple error function profile. Above the upper-

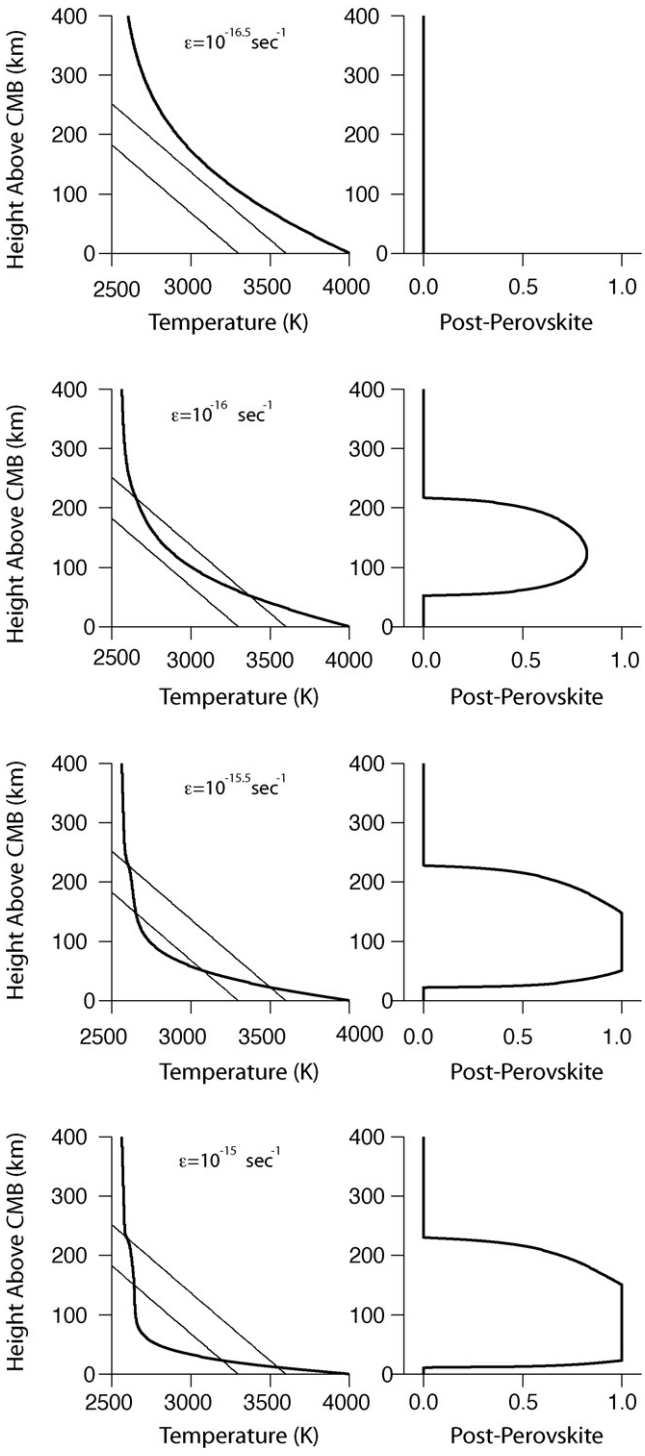

Fig. 4. Effect of strain-rate variations on the form of the solution obtained for the geotherm and fraction of pPv. The computational domain extends to 1000 km above the CMB, however, only the lowermost 400 km are shown. The two-phase region projected onto the T–z plane is outlined by thin lines.

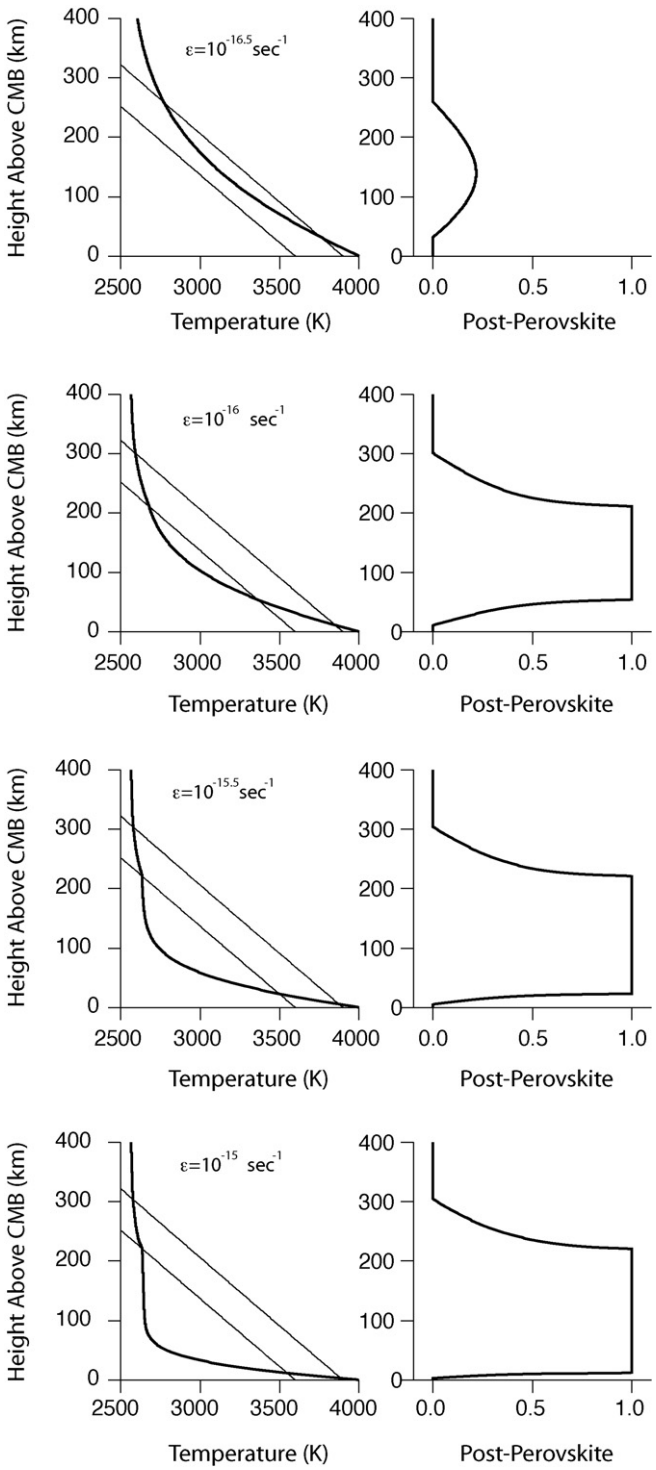

Fig. 5. Same as in Fig. 4, except in these cases the addition of solute X stabilizes pPv (as opposed to stabilizing Pv).

crossing, latent heat deflection of the geotherm assumes the form of a "diffusive pre-cursor" mostly above the two-phase region. The geothermal gradient steepening effect discussed previously for the lower-crossing is not visually obvious for this parameter range.

In all cases in Fig. 4 we observe that the gradient in phase fraction is greatest at the Pv-rich end of the two-phase regions for both the upper and lower crossing. Fig. 5 shows the same models as those in Fig. 4, except that in these cases we suppose that addition of solute X stabilizes pPv by taking $T_{0,cmb}$ =3600 K and $T_{1,cmb}$ =4600 K. The primary difference in the results of this case is that the steepest gradients in phase occur at the pPv-rich end of the two-phase regions, while the gradients are shallower at the Pv-rich side. Another consequence of this change that can be observed is that the diffusive precursor is moved to deeper levels inside the two-phase region for the upper crossing. The cases presented in Figs. 4 and 5 demonstrate that the steepest gradients for both the lower and upper crossing will be produced at the Pv-rich end of the two-phase region(s) when

an increase in X tends to stabilize Pv, and occurs at the pPv-rich end when increase in X stabilizes pPv. Both cases tend toward opposite curvature in pPv abundance, however, both could produce a similar pair of discontinuities.

The deflection of the geotherm by latent heat is an interesting phenomenon, and it is interesting to explore how this behavior changes as more extreme variations of the parameters are considered. Fig. 5 shows the effect of volume change on the form of the solution obtained for the geotherm and fraction of post-perovskite. Because Δs varies in proportion to the volume change (because γ is fixed), the latent heat varies in proportion to Δv. The results illustrate that the temperature change over the diffusive precursor increases as Δv is increased, and the geotherm is deflected to higher temperatures and initially away from the two-phase region. In the case shown in Fig. 5, this causes the part of the geotherm dipping below the two-phase region to become pushed upward into the inside of the two-phase region, such that Pv-free rock never occurs inside the pPv-bearing region. In all of the cases examined, there is no obvious visible effect of the geothermal gradient steepening at the lower crossing and it does not appear to play a significant role in the shape of the geotherm. The positive deflection of the geotherm at the upper boundary actually tends to decrease the thermal gradient beneath it because the CMB temperature is fixed, thus by itself the diffusive precursor has the effect of lowering the CMB heat flux relative to the case where there is no phase transition. Because this effect at the upper crossing increases in proportion to the same factors that cause latent heat geothermal gradient steepening at the lower boundary, the two effects work in opposite directions as the other with respect to affects upon CMB heat flux. Thus the net effect of latent heat for both the upper and lower crossing will be less than one would find by considering the energetics of the lower crossing alone.

Fig. 7 explores the consequences of broadening the two-phase region by increasing the pressure increment across the binary phase loop. The geotherm does not change substantially between these cases, however, the two-phase region grows to the point where the geotherm never fully dips below the Pv-out level and the entire pPv lens becomes mixed in phase. Yet the sharpest gradients in pPv fraction in this case remain at the upper and lower boundaries, and therefore in the case where an increase in X shifts the equilibrium toward Pv, the sharpest gradients in phase would still remain at the boundaries of the two-phase region. Note that the strength of the seismic velocity contrast across the portion of the two-phase region exhibiting the steepest gradients might decrease in this circumstance because the change in phase fraction is smaller. Note also that the highest gradients in pPv at the upper/lower boundaries of the pPv lens become steeper as the two-phase increment increases in size, which would further help to accentuate these upper and lower gradients as seismic features. This is at first sight a very surprising result, because the most simple concept of a two-phase region with phase fraction variations that are approximately linear would lead one to believe that the opposite is true. However, the kind of behavior found here is not without precedent, and was previously described by Stixrude (1997) in the context of shallower mantle phase transitions. Thus the present models verify that the same phenomenon applies to the Pv–pPv phase change: a broad two-phase loop leads to sharper gradients in phase fraction, and we would then expect that broad two-phase regions can produce very sharp seismic discontinuities arising from gradients in phase abundance alone.

6. Discussion and summary

The increasingly ubiquitous findings of a deeper velocity decrease discontinuity in D" that is predicted by the pPv double-crossing model (e.g., Thomas et al., 2004a,b; van der Hilst et al., 2007; Sun et al., 2006; Lay et al., 2006; Kawai et al., 2007a,b) is in contrast to the *a priori* expectation that detecting a velocity decrease – particularly in the presence of realistic levels of seismic noise – should be very difficult (e.g., Flores and Lay, 2005). Negative velocity gradients turn propagated seismic energy downward and de-focus it away from the surface where it would otherwise be recorded as a strong feature in seismograms. Furthermore, velocity decrease discontinuities do not produce unambiguous signals that could readily be detected by a larger scale array (such as the wavefield triplication associated with velocity increase discontinuities). The particular reasons why this lower discontinuity seems easier to detect than it ought to be remains an open question. The present numerical results show that the gradients in phase fraction at the lower crossing are almost always steeper than those associated with the upper crossing, which might help to provide an added sharpness to the lower discontinuity and aid its detection. The reasons for this enhanced sharpness at the lower crossing appear to be simply related to the geometry imposed by a steep geotherm passing through the two phase region just above the CMB.

The findings of the above sections should provide some useful information for interpreting the effects of a two-phase region on the gradient thickness of seismic discontinuities expected from a Pv–pPv phase change. While the appropriate effect cannot be assessed until further progress is made in constraining the phase diagram, the models demonstrate a range of potential complexity and behavior. It is clear from the foregoing results that the width of a two-phase loop alone cannot be considered a good proxy for the seismic velocity "gradient thickness" associated with a phase change. Broadening the two-phase loop may actually cause these gradients to become more sharp, not less sharp, owing to the strongly non-linear variation this broadening induces in the phase fraction. It is worthwhile to briefly consider the increased gradients in phase fraction near the boundaries of the two-phase region in more detail. One simple procedure is to adopt the linearized phase diagram shown in Fig. 8 for purposes of estimating $d\phi/dz$ analytically, a form that is approximately valid for compositions near the end-member of simple binary phase loops. Consider X_{pPv} given by the linear form,

$$X_{pPv} = A_{pPv}(T_0 - T) = A_{pPv}\left[T_{ref} + \frac{\rho g(z_{ref} - z)}{\gamma} - T\right], \tag{42}$$

where A_{pPv} is a constant, and T_0 is the temperature for transformation of the pure end-member component at $X = 0$. T_0 is a function of depth z owing to the pressure dependence of equilibrium and varies as $T_0 = T_{ref} + \rho g(z_{ref} - z)/\gamma$, such that $T_0 = T_{ref}$ when $z = z_{ref}$. A similar expression is adopted for X_{Pv}, namely,

$$X_{Pv} = A_{Pv}(T_0 - T) = A_{Pv}\left[T_{ref} + \frac{\rho g(z_{ref} - z)}{\gamma} - T\right], \tag{43}$$

where A_{Pv} is another constant. Writing $\Delta X = X_{Pv} - X_{pPv}$,

$$\Delta X = \Delta A\left[T_{ref} + \frac{\rho g(z_{ref} - z)}{\gamma} - T\right], \tag{44}$$

where $\Delta A = A_{Pv} - A_{pPv}$. Ignoring the small difference in density between Pv and pPv, an expression for $d\phi/dz$ in this linearized case is given by differentiating the lever rule, Eq. (4), to obtain (following some algebraic manipulation),

$$\frac{d\phi}{dz} = \frac{\phi + (X_{pPv}/\Delta X)}{T_0 - T}\left(\frac{dT}{dz} + \frac{\rho g}{\gamma}\right) = \left(\phi + \frac{X_{pPv}}{\Delta X}\right)\frac{1}{L_\phi}. \tag{45}$$

where $1/L_\phi = (dT/dz + \rho g/\gamma)/(T_0 - T)$ defines a length scale L_ϕ for variations in ϕ. Note that for the upper crossing, the factor $dT/dz + \rho g/\gamma$ is positive, while for the lower crossing it is negative. When the upper and lower two phase regions merge into

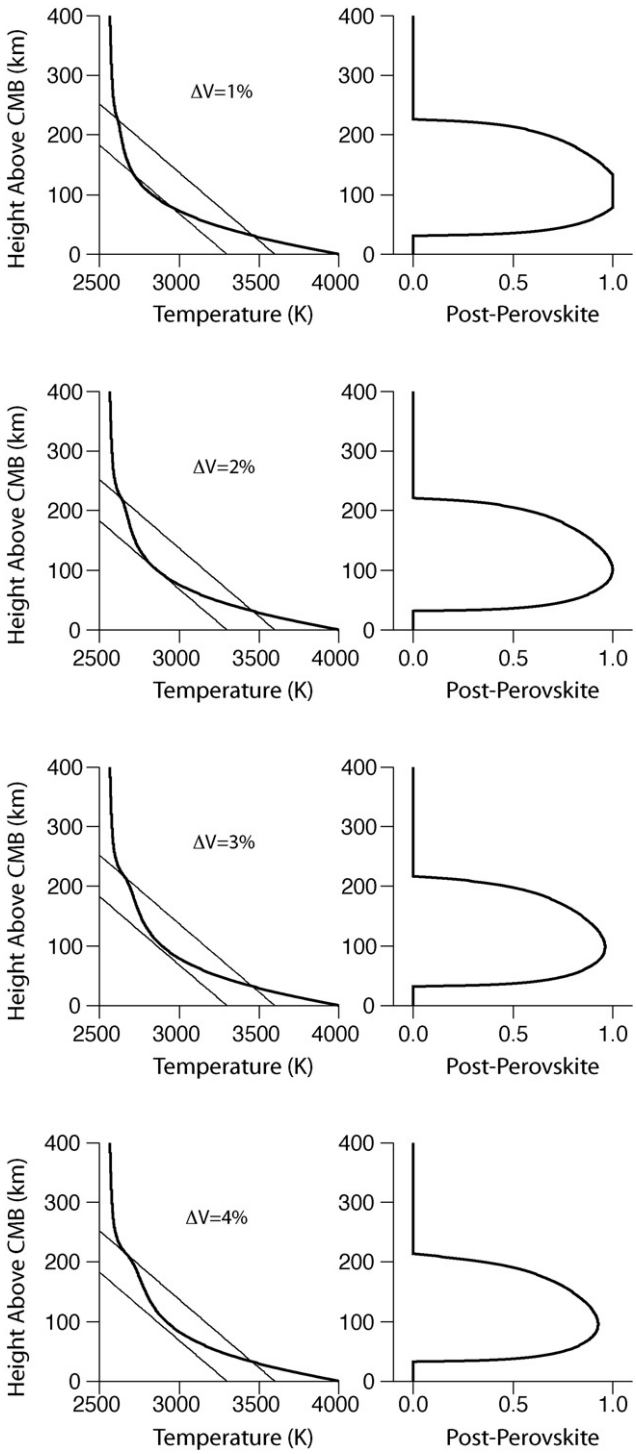

Fig. 6. Effect of volume change on the form of the solution obtained for the geotherm and fraction of post-perovskite. Because Δs varies in proportion to the volume change, a larger latent heat is implied by larger volume changes, causing the geotherm to become significantly deflected at the diffusive precursor.

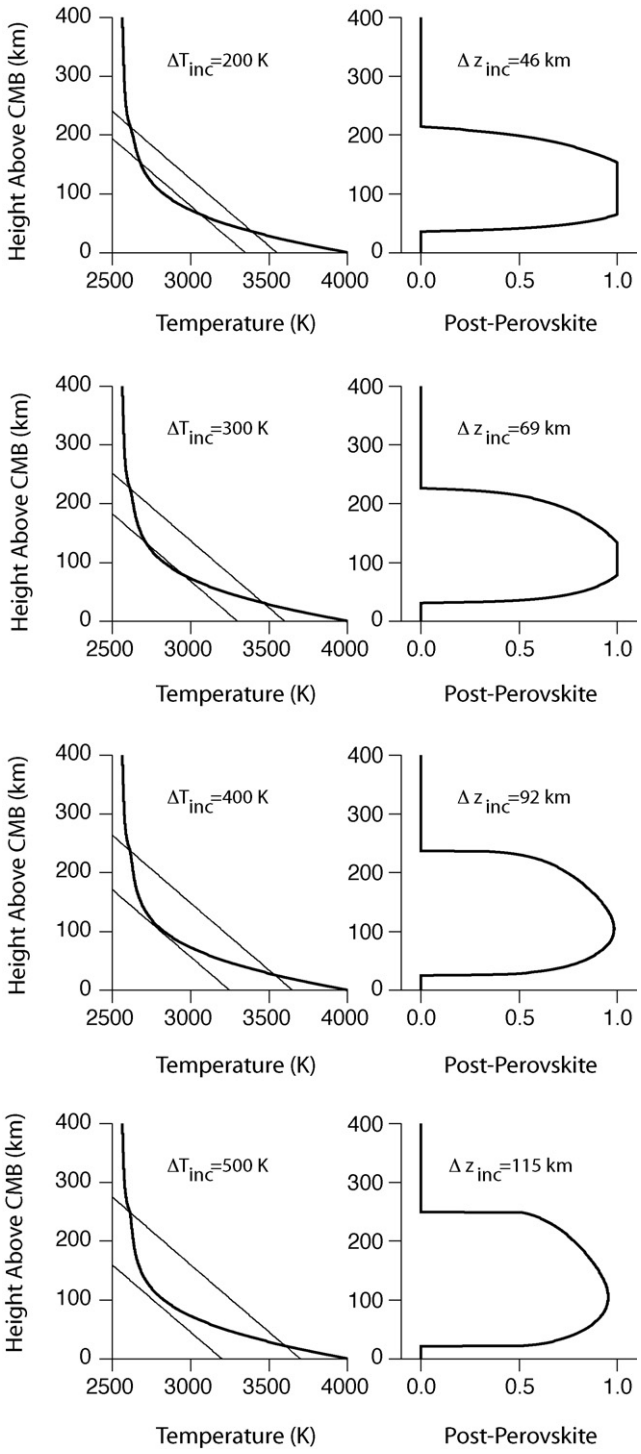

Fig. 7. Effect of temperature and depth increment of the two-phase loop on the form of the solution obtained for the geotherm and fraction of post-perovskite. Note that the highest gradients in pPv at the upper/lower boundaries of the pPv lens become steeper as the increment increases, while the jump in pPv fraction at the boundaries decreases to about 1/2 even as they become sharper.

one another and only a single large mixed phase region exists, the turnaround in phase production – or maximum pPv yield – occurs where $dT/dz = -\rho g/\gamma$, and the geotherm gradient is equal to the phase boundary gradient. There exist two limiting behaviors for the phase variation in this example which depend directly on the parameters governing the phase diagram. If $X_{pPv}/\Delta X >> 1$ (corresponding to an infinitesimally thin binary loop width) then Eq. (45) yields a linear variation in ϕ with depth,

$$\frac{d\phi}{dz'} = \frac{X_{pPv}}{\Delta X}, \tag{46}$$

where $z' = z/L_\phi$ (here L_ϕ is assumed constant for purposes of illustration). On the other hand, if $X_{pPv}/\Delta X << 1$ (corresponding to a very broad binary phase loop) then Eq. (45) yields an exponential

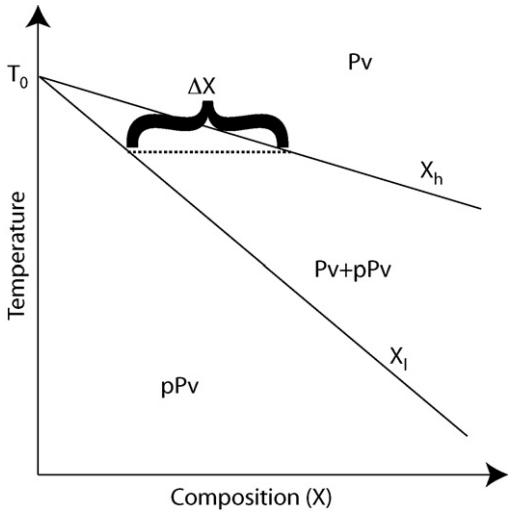

Fig. 8. Sketch of the linearized phase diagram used for purposes of obtaining analytical estimates of $d\phi/dz$. Variables are described in the text.

variation of ϕ with z,

$$\frac{d\log\phi}{dz'} = 1. \tag{47}$$

This simple comparison therefore captures the enhanced nonlinear variation of phase fraction revealed by the numerical solutions (Fig. 6) as the binary phase loop width is increased. Essentially, when the two-phase loop is narrow, the gradient in phase can be linear, but sharp owing to the intrinsic thinness of the co-existence region. On the other hand, when the two-phase region is broad, the phase fraction varies exponentially with depth and therefore can still exhibit sharp gradients where phase fraction varies rapidly over length scales much smaller than the width of the two-phase loop. The result in either case are sharp seismic discontinuities.

It is important to note that phase abundance might not be the only factor influencing the gradient of seismic velocity relative inside a mixed phase Pv–pPv region. Another factor that may be important is the possibility for seismic anisotropy to develop in pPv-bearing regions owing to deformation-induced fabrics (e.g., Iitaka et al., 2004; Tsuchiya et al., 2004b; Oganov et al., 2005; Yamazaki et al., 2006; Merkel et al., 2007). Such fabric transitions might be needed in order to account for the magnitude of seismic velocity changes associated with pPv-related D" discontinuities if the difference in seismic velocity is too small to be accounted for using only isotropic mixtures of Pv and pPv (Murakami et al., 2007). Consider, for example, the case where pPv is rheologically weak relative to Pv under deviatoric stress. In this case, at some critical fraction the pPv phase will become the rheologically dominant phase and the rheology of the two-phase mixture will undergo rapid weakening above this critical fraction of pPv. If this weakening is accompanied by enhanced deformation and subsequent production of a deformation-induced fabric yielding average elastic anisotropy, then a sharp transition in seismic velocity could be produced. Any such rheologically controlled jump in seismic velocity will necessarily be smaller in extent than the equilibrium two-phase region, and is therefore a way of producing velocity jumps that are sharper than those arising from phase fraction variations alone.

A potentially exciting direction for use of these kinds of models in the future is the inverse problem of determining quantities of fundamental importance using constraints from seismology and mineral physics. The study of Lay et al. (2006) was the first to attempt to use pairs of seismic discontinuities attributed to a pPv double-crossing in order to constrain the form of the geotherm in D". It was shown that even if one assumes a simple error function form for the geotherm, the problem is non-unique because the number of uncertain parameters exceeds the number of input data. An exploration of this range of uncertainty was given in that study. Nevertheless, as mineral physics constraints upon thermal conductivity as well as quantities such as the temperature difference between the CMB and Pv–pPv equilibrium points that may be identified with seismic discontinuities improve, the kinds of models described here may be used to perform such inversions. An example from the numerical model used in this study is shown in Fig. 9. This illustrates that if the values for the phase boundary, CMB temperature, and thermal conductivity were well-constrained, then a researcher could in principle take a pair of observed discontinuities and immediately begin to infer the heat flux, temperature changes, and even kinematic factors such as the strain-rate in a given portion of D". Other potential applications might include using models of this kind to produce synthetic seismograms for various parameters, and then comparison of the results with real seismograms in order to contrain the values of some of these quantities using seismic data alone.

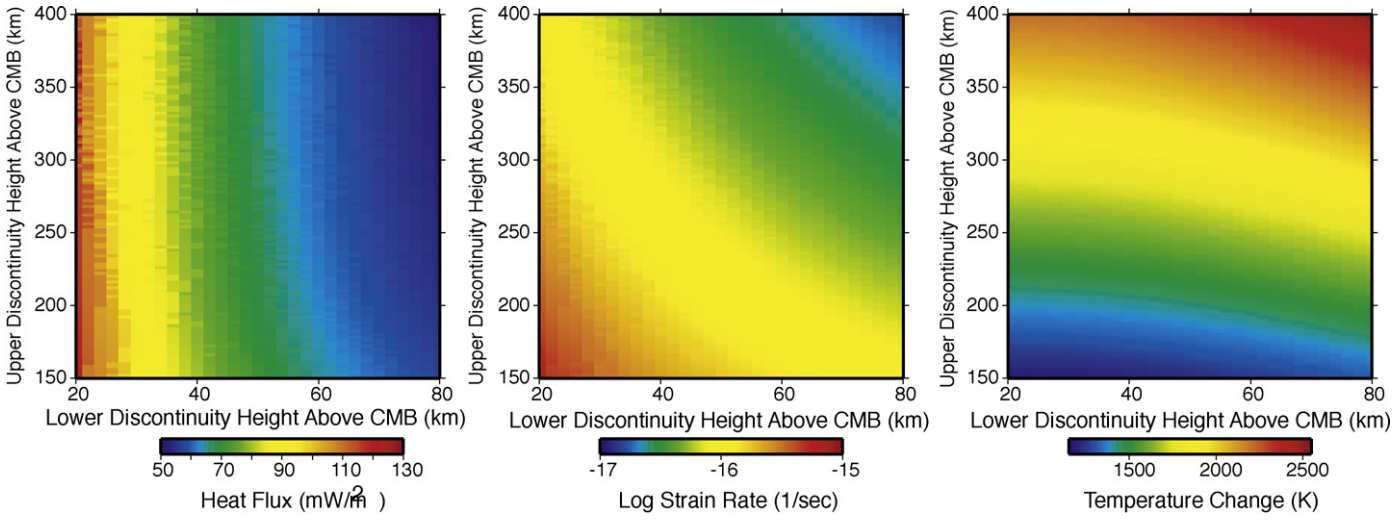

Fig. 9. Illustration of the kind of inverse procedure that could in principle be performed with the numerical model used in this study. In each case, a given pair of upper and lower discontinuity depths is input, and the parameters are then varied so that the steepest gradients in phase match the input depths. These examples show how CMB heat flux, strain-rate, and temperature change across the boundary layer vary as a function of different discontinuity depths.

Acknowledgements

I thank Mark Jellinek, Thorne Lay, and Motohiko Murakami for valuable discussions and I am grateful to Bruce Buffett and Stéphane Labrosse for helpful reviews. This work was supported in part by the Canadian Institute for Advanced Research, Earth Systems Evolution Program. A portion of this manuscript was prepared during a visit to Tohoku University in Sendai, Japan that was supported by the Global C.O.E. program.

References

Akber-Knutston, S., Steinle-Neumann, G., Asimow, P.D., 2005. Effect of al on the sharpness of the $MgSiO_3$ perovskite to postperovskite phase transition. Geophys. Res. Lett. 32, 14303, doi:10.1029/2005GL023192.

Auzende, A.-L., Badro, J., Ryerson, F.J., Weber, P.K., Fallon, S.J., Addad, A., Siebert, J., Fiquet, G., 2008. Element partitioning between magnesium silicate perovskite and ferropericlase: new insights into bulk lower-mantle geochemistry. Earth Planet. Sci. Lett. 269, 164–174, doi:10.1016/j. epsl.2008.02.001.

Avants, M., Lay, T., Russell, S.A., Garnero, E.J., 2006. Shear velocity variation within the D" region beneath the central Pacific. J. Geophys. Res. 111, 05305, doi:10.1029/2004JB003270.

Badro, J., Rueff, J-P., Vankó, G., Monaco, G., Fiquet, G., Guyot, F., 2004. Electronic transitions in perovskite: Possible nonconvecting layers in the lower mantle. Science 305, 383–386.

Braginsky, S.I., Roberts, P.H., 1995. Equations governing convection in Earths core and the geodynamo. Geophys. Astrophys. Fluid Dyn. 79, 1–97.

Buffett, B.A., 2007. A bound on heat flow below a double crossing of the perovskite-postperovskite phase transition. Geophys. Res. Lett. 34, 17302, doi:10.1029/2007GL030930.

Catalli, K., Shim, S.-H., Prakapenka, V., 2009. Thickness and clapeyron slope of the postperovskite boundary. Nature 462, 782–786, doi:10.1038/nature08598.

Dziewonski, A.M., Anderson, D.L., 1981. Preliminary reference Earth model. Phys. Earth Planet. Inter. 25, 297–356.

Flores, C., Lay, T., 2005. The trouble seeing double. Geophys. Res. Lett. 32, 24305.

Helffrich, G., Bina, C.R., 1994. Frequency dependence of the visibility and depths of mantle seismic discontinuities. Geophys. Res. Lett. 21, 2613–2616.

Hernlund, J.W., Labrosse, S., 2007. Geophysically consistent values of the perovskite to post-perovskite transition Clapeyron slope. Geophys. Res. Lett. 34, 05309, doi:10.1029/2006GL028961.

Hernlund, J.W., Thomas, C., Tackley, P.J., 2005. A doubling of the post-perovskite phase boundary and structure of the Earth's lowermost mantle. Nature 434, 882–886, doi:10.1038/nature03472.

Hirose, K., 2006. Postperovskite phase transition and its geophysical implications. Rev. Geophys. 44, R3001, doi:10.1029/2005RG000186.

Hirose, K., Sinmyo, R., Sata, N., Ohishi, Y., 2006. Determination of post-perovskite phase transition in $MgSiO_3$ using Au and MgO pressure standards. Geophys. Res. Lett. 33, 01310.

Houser, C., 2007. Constraints on the presence or absence of post-perovskite in the lowermost mantle from long-period seismology. In: Hirose, K., Brodholt, J., Lay, T., Yuen, D. (Eds.), Post-perovskite: The Last Mantle Phase Transition. American Geophysical Union Monograph, pp. 191–216.

Hutko, A.R., Lay, T., Revenaugh, J., Garnero, E.J., 2008. Anticorrelated seismic velocity anomalies from post-perovskite in the lowermost mantle. Science 320, 1070–1074, doi:10.1126/science.1155822.

Iitaka, T., Hirose, K., Kawamura, K., Murakami, M., 2004. The elasticity of the $MgSiO_3$ post-perovskite phase in the Earth's lowermost mantle. Nature 430, 442–445, doi:10.1038/nature02702.

Kawai, K., Takeuchi, N., Geller, R.J., Fuji, N., 2007a. Possible evidence for a double crossing phase transition in D" beneath Central America from inversion of seismic waveforms. Geophys. Res. Lett. 34, 09314, doi:10.1029/2007GL029642.

Kawai, K., Geller, R.J., Fuji, N., 2007b. D" beneath the Arctic from inversion of shear waveforms. Geophys. Res. Lett. 34, L21305, doi:10.1029/2007GL031517.

Kito, T., Rost, S., Thomas, C., Garnero, E.J., 2007. New insights into the P- and S-wave velocity structure of the D" discontinuity beneath the Cocos plate. Geophys. J. Int. 167, 631–645.

Labrosse, S., 2002. Hotspots, mantle plumes and core heat loss. Earth Planet. Sci. Lett. 199, 147–156.

Lay, T., Hernlund, J., Garnero, E.J., Thorne, M.S., 2006. A post-perovskite lens and D" heat flux beneath the central Pacific. Science 314, 1272–1276, doi:10.1126/science.1133280.

Lay, T., Hernlund, J.W., Buffett, B.A., 2008. Core-mantle boundary heat flow. Nat. Geosci. 1, 25–32.

Mao, W.L., Shen, G., Prakapenka, V.B., Meng, Y., Cambell, A.J., Heinz, D., Shu, J., Hemley, R.J., Mao, H.K., 2004. Ferromagnesian postperovskite silicates in the D" layer of the Earth. Proc. Natl. Acad. Sci. U.S.A. 101, 15867–15869.

McCammon, C., Kantor, I., Narygina, O., Rouquette, J., Ponkratz, U., Sergueev, I., Mezouar, M., Prakapenka, V., Dubrovinsky, L., 2008. Stable intermediate-spin ferrous iron in lower-mantle perovskite. Nat. Geosci. 1, 684–687, doi:10.1038/ngeo309.

Merkel, S., McNamara, A.K., Kubo, A., Speziale, S., Miyagi, L., Meng, Y., Duffy, T.S., Wenk, H., 2007. Deformation of $(Mg,Fe)SiO_3$ post-perovskite and D" anisotropy. Science 316, 1729–1732, doi:10.1126/science.1140609.

Monnereau, M., Yuen, D.A., 2007. Topology of the postperovskite phase transition and mantle dynamics. PNAS 104, 9156–9161.

Morgan, W.J., 1971. Convection plumes in the lower mantle. Nature 230, 42–43.

Murakami, M., Hirose, K., Sata, N., Ohishi, Y., Kawamura, K., 2004. Phase transition of $MgSiO_3$ perovskite in the deep lower mantle. Science 304, 855–858.

Murakami, M., Sinogeikin, S.V., Bass, J.D., Sata, N., Ohishi, Y., Hirose, K., 2007. Sound velocity of $MgSiO_3$ post-perovskite phase: a constraint on the D" discontinuity. Earth Planet. Sci. Lett. 259, 18–23.

Nakagawa, T., Tackley, P.J., 2004. Effects of a perovskite-post perovskite phase change near the core-mantle boundary in compressible mantle convection. Geophys. Res. Lett. 31, 16611.

Nakagawa, T., Tackley, P.J., 2008. Lateral variations in CMB heat flux and deep mantle seismic velocity caused by a thermal-chemical-phase boundary layer in 3D spherical convection. Earth Planet. Sci. Lett. 271, 348–358.

Nakagawa, T., Tackley, P.J., 2005. The interaction between the post-perovskite phase change and a thermo-chemical boundary layer near the core-mantle boundary. Earth Planet. Sci. Lett. 238, 204–216.

Nakagawa, T., Tackley, P.J., 2006. Three-dimensional structures and dynamics in the deep mantle: effects of post-perovskite phase change and deep mantle layering. Geophys. Res. Lett. 33, L11–L12, doi:1029/2006GL025719.

Navrotsky, A., 1994. Physics and Chemistry of Earth Materials. Cambridge University Press.

Oganov, A.R., Ono, S., 2004. Theoretical and experimental evidence for a post-perovskite phase of $MgSiO_3$ in Earth's D" layer. Nature 430, 445–448.

Oganov, A.R., Marto'ak, R., Laio, A., Raiteri, P., Parrinello, M., 2005. Anisotropy of Earth's D" layer and stacking faults in the $MgSiO_3$ post-perovskite phase. Nature 438, 1142–1144, doi:10.1038/nature04439.

Ono, S., Oganov, A.R., 2005. In situ observations of phase transition between perovskite and $CaIrO_3$-type phase in $MgSiO_3$ and pyrolitic mantle composition. Earth Planet. Sci. Lett. 236, 914–932.

Schubert, G., Turcotte, D.L., Olson, P., 2001. Mantle Convection in the Earth and Planets, 1st ed. Cambridge University Press.

Sidorin, I., Gurnis, M., Helmberger, D.V., Ding, X., 1998. Interpreting D" seismic structure using synthetic waveforms computed from dynamic models. Earth Planet. Sci. Lett. 163, 31–41.

Sinmyo, R., Hirose, K., Nishio-Hamane, D., Seto, Y., Fujino, K., Sata, N., Ohishi, Y., 2008. Partitioning of iron between perovskite/postperovskite and ferropericlase in the lower mantle. J. Geophys. Res. 113, B11, doi:10.1029/2008JB005730.

Spera, F.J., Yuen, D.A., Giles, G., 2006. Tradeoffs in chemical and thermal variations in the post-perovskite phase transition: mixed phase regions in the deep lower mantle? Phys. Earth Planet. Int. 159, 234–246, doi:10.1016/j.pepi.2006.07.007.

Stixrude, L., 1997. Structure and sharpness of phase transitions and mantle discontinuities. J. Geophys. Res. 102, 14835–14852.

Sun, D., Helmberger, D., 2008. Lower mantle tomography and phase change mapping. J. Geophys. Res. 113, 10305, doi:10.1029/2007JB005289.

Sun, D., Song, T.-R.A., Helmberger, D., 2006. Complexity of D" in the presence of slab-debris and phase change. Geophys. Res. Lett. 33, L12S07, doi:10.1029/2005GL025384.

Tackley, P.J., Nakagawa, T., Hernlund, J.W., 2007. Influence of the post-perovskite transition on thermal and thermo-chemical mantle convection. In: Lay, T., Yuen, D.A., Hirose, K., Brodholt, J. (Eds.), The Last Phase Transition. American Geophysical Union Monograph.

Tateno, S., Hirose, K., Sata, N., Ohishi, Y., 2007. Solubility of FeO in $(Mg,Fe)SiO_3$ perovskite and the post-perovskite phase transition. Phys. Earth Planet. Inter. 160, 319–325, doi:10.1016/j.pepi.2006.11.010.

Tateno, S., Hirose, K., Sata, N., Ohishi, Y., 2009. Determination of post-perovskite phase transition boundary up to 4400 K and implications for thermal structure in D" layer. Earth Planet. Sci. Lett. 277, 130–136.

Thomas, C., Garnero, E.J., Lay, T., 2004a. High-resolution imaging of lowermost mantle structure under the Cocos plate. J. Geophys. Res. B 109, 08307.

Thomas, C., Kendall, J., Lowman, J., 2004b. Lower-mantle seismic discontinuities and the thermal morphology of subducted slabs. Earth Planet. Sci. Lett. 225, 105–113.

Tsuchiya, T., Tsuchiya, J., Umemoto, K., Wentzcovitch, R.M., 2004a. Phase transition in $MgSiO_3$ perovskite in the earth's lower mantle. Earth Planet. Sci. Lett. 224, 241–248.

Tsuchiya, T., Tsuchiya, J., Umemoto, K., Wentzcovitch, R.M., 2004b. Elasticity of post-perovskite $MgSiO_3$. Geophys. Res. Lett. 31, 14603.

van der Hilst, R.D., de Hoop, M.V., Wang, P., Shim, S.-H., Ma, P., Tenorio, L., 2007. Seismostratigraphy and thermal structure of Earth's core-mantle boundary region. Science 30, 1813–1817, doi:10.1126/science.1137867.

Verhoogen, J., 1965. Phase changes and mantle convection. Philos. Trans. R. Soc. Lond. Ser. A 258, 276–283.

Wookey, J., Stackhouse, S., Kendall, J.-M., Brodholt, J., Price, G.D., 2005. Efficacy of the post-perovskite phase as an explanation of lowermost mantle seismic properties. Nature 438, 1004–1008.

Wysession, M.E., Lay, T., Revenaugh, J., Williams, Q., Garnero, E.J., Jeanloz, R., Kellogg, L.H., 1998. The D" discontinuity and its implications. In: Gurnis, M., Wysession, M.E., Knittle, E., Buffett, B.A. (Eds.), The Core-Mantle Boundary Region. American Geophysical Union Monograph, pp. 273–297.

Yamazaki, D., Yoshino, T., Ohfuji, H., Ando, J., Yoneda, A., 2006. Origin of seismic anisotropy in the D" layer inferred from shear deformation experiments on post-perovskite phase. Earth Planet. Sci. Lett. 252, 372–378.